Failure Profile Analysis of Complex Repairable Systems With Multiple Failure Modes

Qingyu Yang,   Yili Hong,   Yong Chen,   and   Jianjun Shi

Abstract—The relative failure frequency among different failure modes of a production system is referred to as *failure profile* in this paper. Identification of failure profile based on failure-time data collected in the production phase of a system can help pinpoint the bottleneck problems, and provide valuable information for system design evaluation and maintenance management. Major challenges of effective failure profile identification come from time-varying and limited failure-time data. In this paper, the failure profile is estimated by using the maximum likelihood method. In addition, statistical hypothesis testing procedures are proposed to inspect the existence of a dominating failure mode, and possible changes of failure profiles during a production period. The developed methods are illustrated with an automation system of a high throughput screening (HTS) process, and a production process for cylinder heads.

Index Terms—Competing risks, imperfect repair actions, production system, single repairable system, trend-renewal process.

ACRONYMS

TRP	trend-renewal process
ARA	arithmetic reduction of age
ARI	arithmetic reduction of intensity
HTS	high throughput screening
RP	renewal process
HPP	homogeneous Poisson process
NHPP	non-homogeneous Poisson process
ML	maximum likelihood
CI	confidence interval
cdf	cumulative distribution function
pdf	probability density function

NOTATIONS

$N_k(t), N(t)$	number of failures of type k, and that of all types occurring in $(0, t]$, respectively
$T_{k,i}$	the ith failure time of failure type k
$\mathcal{F}_{t-}$	failure-time history up to, but not including, time t
$\gamma_k(t; \boldsymbol{\theta}), \gamma(t; \boldsymbol{\theta})$	conditional intensity functions of $N_k(t)$, and $N(t)$, respectively
$\Gamma_k(t_1, t_2; \boldsymbol{\theta})$	expected cumulative number of failures of type k in time interval $(t_1, t_2]$
$\tilde{\Gamma}_k(t; \boldsymbol{\theta})$	conditional cumulative intensity function
$R(t_1, t_2; \boldsymbol{\theta})$	failure profile in a given time interval $(t_1, t_2]$
$R_k(t_1, t_2; \boldsymbol{\theta})$	kth element of $R(t_1, t_2; \boldsymbol{\theta})$
$\Lambda(t; \boldsymbol{\theta}_\lambda)$	trend function of TRP
$F(z; \boldsymbol{\theta}_F)$	renewal distribution of TRP
$\boldsymbol{\theta}_\lambda, \boldsymbol{\theta}_F$	parameters for the trend function, and renewal distribution, respectively
$\boldsymbol{\theta}_k, \boldsymbol{\theta}$	parameters for failure mode k, and all failure modes, respectively
$L(\boldsymbol{\theta}\|DATA)$	likelihood function for unknown parameter vector $\boldsymbol{\theta}$
$\widehat{\boldsymbol{\theta}}$	ML estimator of $\boldsymbol{\theta}$
$I(\widehat{\boldsymbol{\theta}})$	local information matrix
$R(t_1, t_2; \widehat{\boldsymbol{\theta}})$	estimated failure profile in a given time interval $(t_1, t_2]$
$W_{k,j}$	test statistic for failure mode supremacy
B	test statistic for failure profile change
$g(x)$	a strictly monotonic transformation function to map $[0, 1]$ to $[-\infty, \infty]$

I. INTRODUCTION

A REPAIRABLE system is defined as a system which, after failing to perform one or more of its functions satisfactorily, can be restored to fully satisfactory performance by a method other than replacement of the entire system [1]. Traditional studies on repairable systems focus on modeling failure times, using point process theory as the main tool. For

repairable systems with a single failure mode, widely-used models are the renewal process (RP), where the system is "as good as new" after a repair, and the non-homogeneous Poisson process (NHPP), where the system receives a minimal repair. There are intermediate models between RP and NHPP, which model situations other than perfect and minimal repair conditions. These models include the modulated renewal process [2], the inhomogeneous and modulated gamma processes [3], the modulated power law process [4], and the trend-renewal process (TRP) [5] (a generalization of the models in [3]). The Brown-Proschan model [6], the Kijima's virtual age model [7], and the arithmetic reduction of age (ARA) and arithmetic reduction of intensity (ARI) models [8] are also models that deal with situations in-between perfect and minimal repairs.

In recent years, there has been increasing attention in modeling repairable systems that have different types of failure modes. In a system with multiple failure modes, a repair action is taken if any type of failure event occurs, which is referred to as competing risks. Shaked and Shanthikumar [9] proposed a multi-component imperfect repair model that has dependent life-lengths. Bedford and Lindqvist [10] considered a series system with multiple repairable components in which only the failing component is repaired. Langseth and Lindqvist [11] developed a model for multi-component systems in which failures can be caused by multiple sources. Doyen and Gaudoin [12] presented a point process framework for modeling imperfect repair in a competing risks situation between failure and preventive maintenance. Lindqvist [13] provided a review on statistical methods for repairable systems.

In many applications, the relative failure frequency of different failure modes provides valuable information for system monitoring and maintenance management. For example, a complex manufacturing system may consist of multiple stations in which the failure of each individual station results in failure of the entire system. If the relative failure frequency of one station is statistically larger than other stations, then that station is the system bottleneck. More resources, thus, need to be allocated to that station to improve its reliability and maintainability. The resources and actions include deploying sensor systems to detect failures quickly, increasing inspection frequencies, using components that are more reliable for the repair actions, applying redundancy technology, etc. The relative failure frequency of failure modes in a production system is referred to as the *failure profile*. Failure profile analysis provides a useful tool for system design evaluation and maintenance management for complex systems. Friedman [14] introduced a concept that was similar to failure profile for computer software programs, where the hazard rate was assumed to be constant. With a constant hazard assumption, the hazard rate can be easily estimated based on failure-time data. For most production systems, however, hazard rates are time varying due to system degradation, maintenance and repair, raw material variation, changes of environmental factors, etc. Thus, the constant hazard rate assumption may not be appropriate for production systems.

This paper proposes a general method to analyze the failure profile for a single repairable production system (i.e., failure-time data are collected only from one realization of the repairable system) with imperfect repair actions. Because only one realization can be observed for a single system with multiple failure modes, the intensity functions for each failure mode cannot be estimated nonparametrically [10]. Parametric models thus are used in this paper to build the statistical model of the failure profile. In the literature, the TRP is a general statistical model that is used to model repairable systems with a single failure mode. In this paper, the failure profile is analyzed by applying the TRP model for repairable systems with multiple failure modes. In addition, two hypothesis testing procedures are developed to test whether a dominating failure mode exists during a particular time interval, and whether the failure profiles in two different time intervals are significantly different. The developed methods are demonstrated with a high throughput screening (HTS) automation system, and a production process for cylinder heads.

The rest of the paper is organized as follows. Section II gives the mathematical definition of a failure profile. Section III develops the statistical model of the failure profile based on the TRP model. In Section IV, two hypothesis testing procedures are proposed to study the statistical properties: one is to detect the possible dominating failure mode, and the other is to detect possible changes of failure profiles over time. The proposed methods are applied to two applications of production systems in Section V. Finally, Section VI gives the conclusion.

II. MATHEMATICAL DEFINITION OF FAILURE PROFILE

We consider a single repairable system with K different types of s-independent failure modes. Upon each failure, the system is immediately repaired, then put back into operation. The system is under observation from time $t = 0$ to a predetermined time τ. Let $N_k(t)$ be the counting process associated with the system failure of type k, $k = 1, 2, \ldots, K$; $N_k(t)$ records the number of events of type k occurring in the time interval $(0, t]$. The number of failures of all types occurring in $(0, t]$, denoted by $N(t)$, is calculated as $N(t) = \sum_{k=1}^{K} N_k(t)$. The observed failure times for failure type k are denoted by $T_{k,i}$, $i = 1, 2, \cdots N_k(\tau)$, $k = 1, 2, \cdots K$. In particular, $0 < T_{k,1} < T_{k,2} <, \ldots, < T_{k,N_k(\tau)} < \tau$, indicating the ordered failure times for failure type k.

Let $\mathcal{F}_{t^-} = \{T_{k,i}; i = 1, 2, \cdots, N_k(t^-) \text{ and } k = 1, 2, \cdots, K\}$ be the failure history up to, but not including, time t, where $N_k(t^-)$ denotes the number of failures of type k that occur in $(0, t)$. In other words, $\mathcal{F}_{t^-}$ contains all of the information about the failure times and failure types prior to time t. The conditional intensity function of the counting process $N_k(t)$, denoted as

$$\gamma_k(t; \boldsymbol{\theta}_k)$$
$$= \lim_{\Delta t \to 0} \frac{\Pr(\text{an event of type } k \text{ occurs in} [t, t + \Delta t] | \mathcal{F}_{t^-})}{\Delta t}.$$
$$(1)$$

The quantity $\gamma_k(t; \boldsymbol{\theta}_k)\Delta t$ gives an approximation of the probability that an event of type k occurs in $[t, t + \Delta t)$, given the failure history $\mathcal{F}_{t^-}$. Similarly, let $\gamma(t; \boldsymbol{\theta}) = \sum_{k=1}^{K} \gamma_k(t; \boldsymbol{\theta}_k)$ where $\boldsymbol{\theta} = (\boldsymbol{\theta}_1^T, \ldots, \boldsymbol{\theta}_K^T)^T$. The quantity $\gamma(t; \boldsymbol{\theta})\Delta t$ approximates the probability of a failure of all types in $[t, t + \Delta t)$.

Based on (1), the expected cumulative number of failures of type k in the time interval $(t_1, t_2]$, denoted by $\Gamma_k(t_1, t_2; \boldsymbol{\theta}_k)$, $k = 1, 2, \cdots, K$, is calculated as

$$
\begin{aligned}
\Gamma_k(t_1, t_2; \boldsymbol{\theta}_k) &= \mathbf{E}\left(\int_{t_1}^{t_2} \gamma_k(s; \boldsymbol{\theta}_k)ds\right) \\
&= \mathbf{E}\left(\int_0^{t_2} \gamma_k(s; \boldsymbol{\theta}_k)ds\right) - \mathbf{E}\left(\int_0^{t_1} \gamma_k(s; \boldsymbol{\theta}_k)ds\right) \\
&= \mathbf{E}\left(\tilde{\Gamma}_k(t_2; \boldsymbol{\theta}_k)\right) - \mathbf{E}\left(\tilde{\Gamma}_k(t_1; \boldsymbol{\theta}_k)\right)
\end{aligned}
\tag{2}
$$

where

$$
\tilde{\Gamma}_k(t; \boldsymbol{\theta}_k) = \int_0^t \gamma_k(s; \boldsymbol{\theta}_k)ds.
\tag{3}
$$

Note that $\Gamma_k(t_1, t_2; \boldsymbol{\theta}_k)$ is a deterministic function of unknown parameters $\boldsymbol{\theta}_k$. Similarly, let $\Gamma(t_1, t_2; \boldsymbol{\theta}) = \sum_{k=1}^K \Gamma_k(t_1, t_2; \boldsymbol{\theta}_k)$. Then $\Gamma(t_1, t_2; \boldsymbol{\theta})$ is the expected number of failures of all types in $(t_1, t_2]$. Based on $\Gamma_k(t_1, t_2; \boldsymbol{\theta}_k)$, and $\Gamma(t_1, t_2; \boldsymbol{\theta})$, the formal definition of failure profile is given as follows.

Definition 1 (Failure Profile): For a repairable system with K types of failure modes, the failure profile in a given time interval $(t_1, t_2]$, denoted by $R(t_1, t_2; \boldsymbol{\theta})$, is a vector defined as

$$
\begin{aligned}
&R(t_1, t_2; \boldsymbol{\theta}) \\
&= \left[\frac{\Gamma_1(t_1, t_2; \boldsymbol{\theta}_1)}{\Gamma(t_1, t_2; \boldsymbol{\theta})}, \ldots, \frac{\Gamma_k(t_1, t_2; \boldsymbol{\theta}_k)}{\Gamma(t_1, t_2; \boldsymbol{\theta})}, \ldots, \frac{\Gamma_K(t_1, t_2; \boldsymbol{\theta}_K)}{\Gamma(t_1, t_2; \boldsymbol{\theta})}\right]^T.
\end{aligned}
\tag{4}
$$

The kth element of $R(t_1, t_2; \boldsymbol{\theta})$, denoted by $R_k(t_1, t_2; \boldsymbol{\theta})$, represents the relative failure frequency for failure mode k. Note that $\sum_{k=1}^K R_k(t_1, t_2; \boldsymbol{\theta}) = 1$.

III. Statistical Modeling of Failure Profile Based on TRP

To make a statistical inference for the failure profile, a statistical model is generally needed to model the probabilistic mechanisms of system failures. In the literature, the RP and NHPP models are commonly used to model a repairable system with a single failure mode. The RP model assumes that the repaired system is "as good as new, " and the NHPP model assumes that the repaired system is "as bad as the old."

For most applications, however, the RP and NHPP models may not be appropriate because the repair is neither perfect nor minimal. In the literature, some general models not only include the RP and NHPP models as two extreme cases, but also capture situations in-between. Among these models, the Brown-Proschan model [6] assumes that the probability that a system returns to "as good as new" after each repair is a constant during the entire life of the system. In practice, however, it is more likely that the probability that the system returns to "as good as new" after each repair varies as a function of the system's age. The Kijima's virtual age model [7] requires information for each repair. This information, however, is not available in our motivating examples. The ARA and ARI models [8]
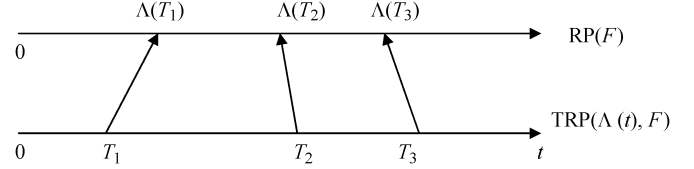

Fig. 1.   Illustration of the TRP model.

are very flexible and powerful. However, there is no clear evidence that there is autocorrelation between repairs (required in ARA or ARI models) in our motivating examples. In contrast, the TRP model [5] is flexible, and has meaningful interpretations. Thus, in this paper, the failure profile is analyzed based on the TRP model.

A. Introduction to Trend-Renewal Process

The TRP is a statistical model for repairable systems with a single type of failure [5]. The main idea of TRP is to generalize the following well known property of the NHPP. Let $\lambda(t)$ be an intensity function. The cumulative intensity function of $\lambda(t)$ is defined by $\Lambda(t) = \int_0^t \lambda(u)du$. If the failure times of a repairable system, denoted by $T_1, T_2, \ldots$, is an NHPP with intensity function $\lambda(t)$, then the time-transformed process $\Lambda(T_1), \Lambda(T_2), \ldots$, denoted by HPP(1), is a homogeneous Poisson process (HPP) with event rate equaling one. The TRP generalizes HPP(1) to be any renewal process $RP(F)$, where F is a cumulative distribution function (cdf). Thus, a TRP model is characterized by $\Lambda(t; \boldsymbol{\theta}_\lambda)$, and $F(z; \boldsymbol{\theta}_F)$.

Formally, a TRP is defined as follows. Let $\Lambda(t; \boldsymbol{\theta}_\lambda)$ be a nonnegative monotone increasing function of t, which satisfies three conditions: $\Lambda(t; \boldsymbol{\theta}_\lambda) < \infty$ for each $t \geq 0$, $\Lambda(\infty; \boldsymbol{\theta}_\lambda) = \infty$, and $\Lambda(0; \boldsymbol{\theta}_\lambda) = 0$. The process $T_1, T_2, \ldots$, is a TRP if $Z_i = \Lambda(T_i; \boldsymbol{\theta}_\lambda) - \Lambda(T_{i-1}; \boldsymbol{\theta}_\lambda)$ $(i = 1, 2, \ldots,$ and $T_0 = 0)$ are s-independent and identically distributed (iid) random variables with cdf equaling $F(z; \boldsymbol{\theta}_F)$.)

In addition, the renewal distribution $F(z; \boldsymbol{\theta}_F)$ in a TRP needs to satisfy the following two conditions [5]: $F(z; \boldsymbol{\theta}_F)$ is the cdf of a positive random variable, in particular, $F(0; \boldsymbol{\theta}_F) = 0$; and the expectation of the distribution equals one.

The probability density function (pdf) of Z_i is denoted by $f(z; \boldsymbol{\theta}_F)$, and the hazard function is denoted by $h(z; \boldsymbol{\theta}_F)$. In particular, $h(z; \boldsymbol{\theta}_F) = f(z; \boldsymbol{\theta}_F)/[1 - F(z; \boldsymbol{\theta}_F)]$. The cumulative hazard function is defined by $H(z; \boldsymbol{\theta}_F) = \int_0^z h(s; \boldsymbol{\theta}_F)ds$.

Fig. 1 illustrates the definition of the TRP. For special cases, a TRP is an NHPP with intensity function $\lambda(t)$, if the trend function is $\Lambda(t) = \int_0^t \lambda(u)du$, and the renewal distribution is $F(z; \boldsymbol{\theta}_F) = 1 - e^{-z}$ (i.e., the cdf of a unit exponential distribution). More specifically, a TRP is an $HPP(\lambda)$ if the trend function is $\Lambda(t; \boldsymbol{\theta}_\lambda) = \lambda t$ with a constant λ, and the renewal distribution is $F(z; \boldsymbol{\theta}_F) = 1 - e^{-z}$. In contrast, a TRP is a RP with renewal distribution F if the trend function is the identity function, and the renewal distribution is F. Thus, the TRP model includes both the RP model (i.e., the repairs are perfect) and the NHPP model (i.e., the repairs are minimal) as two special cases. When the repair is neither perfect nor minimal, the TRP model provides flexible models that can capture the RP, NHPP, and situations in-between [6].

B. Parametric Forms for Trend Function and Renewal Distribution

In practice, the power law function is generally chosen as the trend function in the TRP model. In particular, the power law function is

$$\lambda(t; \boldsymbol{\theta}_\lambda) = \frac{\beta}{\eta}\left(\frac{t}{\eta}\right)^{\beta-1} \tag{5}$$

where $\boldsymbol{\theta}_\lambda = (\beta, \eta)^T$ is the parameter vector.

The Weibull distribution and lognormal distribution are commonly used as renewal distributions of the TRP model. The Weibull and lognormal distributions are from the log-location-scale family of distributions [15], and are commonly used failure-time distributions. The cdf, and pdf of the Weibull distribution are respectively given as

$$F(z; \boldsymbol{\theta}_F) = \Phi_{\mathrm{sev}}\left[\frac{\log(z) - \mu}{\sigma}\right], \tag{6}$$

$$f(z; \boldsymbol{\theta}_F) = \frac{1}{\sigma z}\phi_{\mathrm{sev}}\left[\frac{\log(z) - \mu}{\sigma}\right] \tag{7}$$

where $\Phi_{\mathrm{sev}}(x) = 1 - \exp[-\exp(x)]$, and $\phi_{\mathrm{sev}}(x) = \exp[x - \exp(x)]$ are the cdf, and pdf of the standard smallest extreme value distribution, respectively. Here μ is the location parameter, and σ is the scale parameter. For the lognormal distribution, the standard s-normal distribution cdf and pdf, denoted respectively by Φ_{nor} and ϕ_{nor}, are used to replace Φ_{sev} and ϕ_{sev} in both (6) and (7), respectively. Because the expectation of the renewal distribution in the TRP model is restricted to one, we only need one parameter for the renewal distribution in both (6) and (7), which is $\boldsymbol{\theta}_F = \sigma$. The location parameter μ in (6) and (7) can be calculated as follows. For the Weibull distribution, by setting the expectation (i.e., $\exp(\mu)\mathrm{Gamma}(1+\sigma)$) to 1, we obtain $\mu = -\log[\mathrm{Gamma}(1 + \sigma)]$. Similarly, for the lognormal distribution, the location parameter μ is obtained as $\mu = -\sigma^2/2$ by setting the expectation to 1, i.e., $\exp(\mu + \sigma^2/2) = 1$.

C. Failure Profile Estimation Based on TRP

In this paper, the TRP model is applied to model single repairable systems with multiple failure modes. In the literature, different failure modes of a repairable system are generally assumed to be s-independent. Tsiatis [16] showed that, for a single repairable system, it is impossible to distinguish between s-dependent and s-independent structures nonparametrically based only on failure-time data and failure mode information. Bedford and Lindqvist [10] proved that a dependent structure is identifiable for repairable systems under a partial repair assumption. The partial repair assumption, however, is difficult to verify for a single repairable system that generally has limited data. In our motivating examples, different failure modes arise from different stations of the production systems. As these stations do not share mechanics and are maintained separately, it is reasonable to assume they fail s-independently. Thus, we assume s-independent failure modes. Each type of failure mode is modeled

separately by a TRP model. In particular, the conditional intensity function for failure mode k in (1) is given as

$$\gamma_k(t; \boldsymbol{\theta}_k) = h\left[\Lambda(t; \boldsymbol{\theta}_{\lambda_k}) - \Lambda(T_{k,N_k(t^-)}; \boldsymbol{\theta}_{\lambda_k}); \boldsymbol{\theta}_{F_k}\right]\lambda(t; \boldsymbol{\theta}_{\lambda_k}),$$
$$k = 1, 2, \ldots, K \quad (8)$$

where $\boldsymbol{\theta}_k = (\boldsymbol{\theta}_{F_k}^T, \boldsymbol{\theta}_{\lambda_k}^T)^T$ is the parameter vector for failure mode k. $T_{k,N_k(t^-)}$ denotes the latest event time prior to time t for type k. $T_{k,N_k(t^-)} = 0$ if no event of type k occurs prior to time t. In our motivating examples, it is adequate to use the same functional forms of h and Λ for all failure modes, with different values of parameters. It is worthy to notice that it is possible to allow each failure mode to have different functional forms for h and Λ. For the intensity function in (8), the quantity $\tilde{\Gamma}_k(t; \boldsymbol{\theta}_k)$ in (3) is calculated by

$$\begin{aligned}
&\tilde{\Gamma}_k(t; \boldsymbol{\theta}_k) \\
&= \int_0^t \gamma_k(s; \boldsymbol{\theta}_k)ds \\
&= \int_{T_{k,N_k(t^-)}}^t \gamma_k(s; \boldsymbol{\theta}_k)ds \\
&\quad + \mathbf{1}_{[N_k(t^-)>0]}\sum_{i=1}^{N_k(t^-)}\int_{T_{k,i-1}}^{T_{k,i}}\gamma_k(s; \boldsymbol{\theta}_k)ds \\
&= H\left[\Lambda(t; \boldsymbol{\theta}_{\lambda_k}) - \Lambda(T_{k,N_k(t^-)}; \boldsymbol{\theta}_{\lambda_k}); \boldsymbol{\theta}_{F_k}\right] \\
&\quad + \mathbf{1}_{[N_k(t^-)>0]}\sum_{i=1}^{N_k(t^-)}H\left[\Lambda(T_{k,i}; \boldsymbol{\theta}_{\lambda_k})\right. \\
&\qquad\qquad\qquad\qquad\left. -\Lambda(T_{k,i-1}; \boldsymbol{\theta}_{\lambda_k}); \boldsymbol{\theta}_{F_k}\right]
\end{aligned}$$

where $\mathbf{1}_{(\bullet)}$ is an indicator function, $T_{k,0} = 0$, and $H(z; \boldsymbol{\theta}_{F_k}) = \int_0^z h(s; \boldsymbol{\theta}_{F_k})ds$.

The likelihood of parameter $\boldsymbol{\theta}$ in the general model (1), is calculated as [17]

$$\begin{aligned}
&L(\boldsymbol{\theta}|DATA) \\
&= \prod_{k=1}^K\left[\prod_{i=1}^{N_k(\tau)}\gamma_k(T_{k,i}; \boldsymbol{\theta}_k)\right] \times \exp\left[-\int_0^\tau \gamma(u; \boldsymbol{\theta})du\right] \quad (9)
\end{aligned}$$

where $\gamma(t; \boldsymbol{\theta}) = \sum_{k=1}^K \gamma_k(t; \boldsymbol{\theta}_k)$. Substituting (8) into (9), the likelihood function for unknown parameter vector $\boldsymbol{\theta}$, where $\boldsymbol{\theta} = (\boldsymbol{\theta}_1^T, \cdots, \boldsymbol{\theta}_K^T)^T$, is given in (10), shown at the bottom of the next page. The maximum likelihood (ML) estimate of $\boldsymbol{\theta}$, denoted by $\widehat{\boldsymbol{\theta}}$, is the value of $\boldsymbol{\theta}$ that maximizes $L(\boldsymbol{\theta}|DATA)$. Because the failure modes are assumed to be s-independent, the maximization of (10) can be implemented separately for each failure mode. The log-likelihood function is denoted by $\mathrm{L}(\boldsymbol{\theta}) = \log[L(\boldsymbol{\theta}|DATA)]$. The local information matrix is the negative of the Hessian matrix evaluated at $\boldsymbol{\theta} = \widehat{\boldsymbol{\theta}}$, i.e.,

$$I(\widehat{\boldsymbol{\theta}}) = -\left.\frac{\partial^2 \mathrm{L}(\boldsymbol{\theta})}{\partial\boldsymbol{\theta}\partial\boldsymbol{\theta}^T}\right|_{\boldsymbol{\theta}=\widehat{\boldsymbol{\theta}}}. \tag{11}$$

As we consider a single repairable system in which failure-time data are collected from only one realization of the repairable system, we can not assume the number of systems goes to infinity (i.e., $n \to \infty$) to obtain the asymptotic distribution of $\widehat{\boldsymbol{\theta}}$. The asymptotic distribution of the ML estimator $\widehat{\boldsymbol{\theta}}$ in (10), however, can be obtained when the length of the observation period goes to infinity (i.e., $\tau \to \infty$). Based on the results in Svensson [18], the asymptotic normality of $\widehat{\boldsymbol{\theta}}$ holds under some mild conditions, which are generally imposed in ML theory. As noted in Lindqvist *et al.* [5], Svensson's results can be applied to the TRP model. Although the variance-covariance matrix for $\widehat{\boldsymbol{\theta}}$ in Svensson [18] is obtained by the estimated quadratic variation process, the local information matrix in (11) is asymptotically equivalent to the estimated quadratic variation process. As the local information is easy to calculate, it is used in this paper.

The ML estimator $\widehat{\boldsymbol{\theta}}$ is asymptotically distributed with multivariate normal distribution

$$\widehat{\boldsymbol{\theta}} \overset{\cdot}{\sim} N\left[\boldsymbol{\theta}, \Sigma(\widehat{\boldsymbol{\theta}})\right], \quad \text{where } \Sigma(\widehat{\boldsymbol{\theta}}) = I^{-1}(\widehat{\boldsymbol{\theta}}). \qquad (12)$$

Here, $\overset{\cdot}{\sim}$ stands for asymptotically distributed. Large-sample confidence intervals (CIs) for unknown parameters can be constructed by using the asymptotic result in (12). Based on the invariance property of the ML estimator [19], the ML estimate of the failure profile is obtained by substituting $\widehat{\boldsymbol{\theta}}$ into (4). Specifically, the estimated failure profile in the time interval $(t_1, t_2]$ for $t_1, t_2 \leq \tau$, denoted by $R(t_1, t_2; \widehat{\boldsymbol{\theta}})$, is given as

$$R(t_1, t_2; \hat{\boldsymbol{\theta}}) = \left[\frac{\Gamma_1(t_1, t_2; \hat{\boldsymbol{\theta}}_1)}{\Gamma(t_1, t_2; \hat{\boldsymbol{\theta}})}, \cdots, \frac{\Gamma_k(t_1, t_2; \hat{\boldsymbol{\theta}}_k)}{\Gamma(t_1, t_2; \hat{\boldsymbol{\theta}})}, \right.$$
$$\left. \cdots, \frac{\Gamma_K(t_1, t_2; \hat{\boldsymbol{\theta}}_K)}{\Gamma(t_1, t_2; \hat{\boldsymbol{\theta}})} \right]^T \qquad (13)$$

where the kth element of $R(t_1, t_2; \boldsymbol{\theta})$ is estimated by $R_k(t_1, t_2; \hat{\boldsymbol{\theta}})$.

D. Simulation Study on the Performance of the Asymptotic Result

We conducted simulation studies to see the effect of sample size on the performance of the asymptotic result in (12). As the likelihood in (10) is separable for each failure mode, we only need to conduct simulation based on one failure mode. For each

trial, a series of events are simulated, and the ML estimates are obtained as $(\hat{\beta}, \hat{\eta}, \hat{\sigma})^T$, where β and η are unknown parameters for the power law trend function, and σ is the unknown parameter for the renewal distribution. In addition, the approximate 95% CIs for parameters β, η, and σ are constructed respectively. The coverage probability of the CI procedures is estimated by using 10,000 trials. If the asymptotic results work well, the estimated coverage probability should be close to the nominal one. Fig. 2 shows the estimated coverage probability of the approximate CI procedures for parameters in the TRP model under four different settings. In each setting, 10,000 trials are simulated for each fixed follow-up time τ; CIs for the parameters are constructed; and the estimated coverage probability is plotted against the average number of observations in Fig. 2.

The simulation results show that the asymptotic result in (12) works well when the number of observations from each failure mode is more than 100. The asymptotic result works reasonable well when the number of observations is around 20. The performance is not very good when the number of observations is below 10, as the coverage probability for the CI procedure for the parameter tends to be less than the nominal one.

IV. HYPOTHESIS TESTS FOR FAILURE PROFILES

Based on the statistical model of the failure profile established in Section III, statistical testing procedures are developed in this section to investigate the statistical properties of the failure profile. In Section IV-A, the existence of a failure mode whose failure frequency is s-larger than all others is investigated. In Section IV-B, possible changes in the failure profile during the production phase of the system are studied.

A. Test of Failure Mode Supremacy

For repairable systems with multiple failure modes, if the relative failure frequency of a failure mode is s-larger than that of other failure modes, more attention needs to be paid to this failure mode in both the design and maintenance stages. A s-testing procedure is developed to find the possible superior failure mode. Formally, given time interval $(t_1, t_2]$, to test whether the kth failure mode has a superior relative failure frequency, the test hypothesis is defined as

$$H_0 : R_k(t_1, t_2; \boldsymbol{\theta}) \leq \max \left\{ R_j(t_1, t_2; \boldsymbol{\theta}); j \neq k \right\} \text{ vs}$$
$$H_1 : R_k(t_1, t_2; \boldsymbol{\theta}) > \max \left\{ R_j(t_1, t_2; \boldsymbol{\theta}); j \neq k \right\}. \quad (14)$$

$$L(\boldsymbol{\theta}|DATA) = \prod_{k=1}^{K} \left\{ \prod_{i=1}^{N_k(\tau)} h\left[\Lambda\left(T_{k,i}; \boldsymbol{\theta}_{\lambda_k}\right) - \Lambda\left(T_{k,i-1}; \boldsymbol{\theta}_{\lambda_k}\right); \boldsymbol{\theta}_{F_k} \right] \lambda\left(T_{k,i}; \boldsymbol{\theta}_{\lambda_k}\right) \right\}$$
$$\times \exp\left(-\int_0^{\tau} \sum_{k=1}^{K} \left\{ h\left[\Lambda(t; \boldsymbol{\theta}_{\lambda_k}) - \Lambda\left(T_{k,N_k(t-)}; \boldsymbol{\theta}_{\lambda_k}\right); \boldsymbol{\theta}_{F_k} \right] \lambda(t; \boldsymbol{\theta}_{\lambda_k}) \right\} dt \right). \quad (10)$$
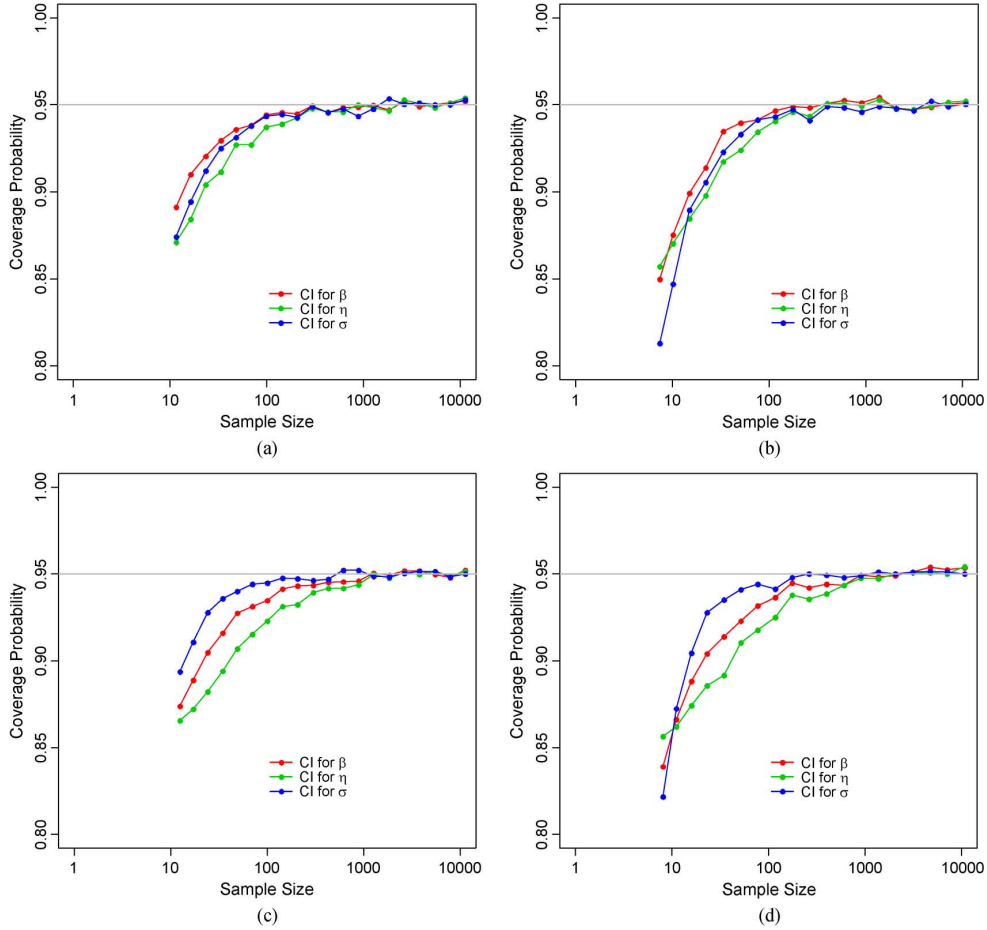
Fig. 2. Estimated coverage probability of the approximate CI procedures for parameters in the TRP model. (a) Weibull ($\sigma = 1.2$), Power law ($\beta = 1.5, \eta = 1$) (b) Weibull ($\sigma = 1.2$), Power law ($\beta = .9, \eta = 1$). (c) Lognormal ($\sigma = 1.2$), Power law ($\beta = 1.5, \eta = 1$). (d) Lognormal ($\sigma = 1.2$), Power law ($\beta = .9, \eta = 1$).

The test hypothesis (14) is known as the intersection-union test in Silvapulle and Sen [20], and it can be further written as

$$H_0 : \bigcup_{j \neq k} \{R_k(t_1, t_2; \boldsymbol{\theta}) \leq R_j(t_1, t_2; \boldsymbol{\theta})\} \text{ vs}$$

$$H_1 : \bigcap_{j \neq k} \{R_k(t_1, t_2; \boldsymbol{\theta}) > R_j(t_1, t_2; \boldsymbol{\theta})\}.$$

The development of the testing procedure for (14) relies on $K - 1$ individual tests:

$$H_{0,j} : R_k(t_1, t_2; \boldsymbol{\theta}) \leq R_j(t_1, t_2; \boldsymbol{\theta}) \text{ vs } H_{1,j} : R_k(t_1, t_2; \boldsymbol{\theta})$$
$$> R_j(t_1, t_2; \boldsymbol{\theta}), \quad \text{for } j = 1, \ldots, K, j \neq k. \quad (15)$$

Based on Proposition 5.3.1 of [20], the H_0 of test (14) is rejected at the α level (i.e., the kth failure mode has a superior relative failure frequency) iff all the individual tests in [15] are rejected at the α level. The p-value for test (14) is the maximum of the p-values from the $K - 1$ individual test in [15]. More details on the intersection-union test can be found in Section V-C of [20].

Normal approximation is used in the tests, i.e., the test statistic is constructed as the estimate divided by its estimated

standard error. As the asymptotic result in (12) is applied, all the distributional results of the hypothesis testing are asymptotic. Note that the range of $R_k(t_1, t_2; \boldsymbol{\theta})$ is bounded by zero and one, while the domain of a s-normal random variable is from $-\infty$ to ∞. Thus, to improve the performance of the normal approximation, transformations are often used in practice [15] to map the range of $R_k(t_1, t_2; \boldsymbol{\theta})$ from [0,1] to $[-\infty, \infty]$. With a strictly monotonic transformation function $g(x)$ being applied, the tests in (15) are equivalent to

$$H_{0,j} : g[R_k(t_1, t_2; \boldsymbol{\theta})] \leq g[R_j(t_1, t_2; \boldsymbol{\theta})] \text{ vs}$$
$$H_{1,j} : g[R_k(t_1, t_2; \boldsymbol{\theta})] > g[R_j(t_1, t_2; \boldsymbol{\theta})]$$
$$j = 1, \ldots, K, j \neq k. \quad (16)$$

Here $g(x)$ is chosen as the logit function, i.e., $g(x) = \log[x/(1 - x)]$, where $0 < x < 1$.

Note that the individual tests in (16) are one-sided tests. The test statistics $W_{k,j}$ for individual test j is defined by

$$W_{k,j} = \frac{D_{k,j}(t_1, t_2; \widehat{\boldsymbol{\theta}})}{\left\{U^T I^{-1}(\widehat{\boldsymbol{\theta}}) U\right\}^{\frac{1}{2}}} \quad (17)$$

where $D_{k,j}(t_1, t_2; \widehat{\boldsymbol{\theta}}) = g[R_k(t_1, t_2; \widehat{\boldsymbol{\theta}})] - g[R_j(t_1, t_2; \widehat{\boldsymbol{\theta}})]$, and

$$U = \frac{\partial R_k(t_1, t_2; \widehat{\boldsymbol{\theta}})/\partial \widehat{\boldsymbol{\theta}}}{R_k(t_1, t_2; \widehat{\boldsymbol{\theta}}) \left[1 - R_k(t_1, t_2; \widehat{\boldsymbol{\theta}})\right]}$$
$$- \frac{\partial R_j(t_1, t_2; \widehat{\boldsymbol{\theta}})/\partial \widehat{\boldsymbol{\theta}}}{R_j(t_1, t_2; \widehat{\boldsymbol{\theta}}) \left[1 - R_j(t_1, t_2; \widehat{\boldsymbol{\theta}})\right]}$$

The calculation of $\partial R_k(t_1, t_2; \hat{\boldsymbol{\theta}})/\partial \hat{\boldsymbol{\theta}}$ is given in the Appendix. Proposition 1 as follows gives the decision rule to test the individual hypothesis $H_{0,j}$ in (16). The detailed proof is provided in the Appendix.

Proposition 1: The individual hypothesis $H_{0,j}$ in (16) is rejected if $W_{k,j} > z_\alpha$, where z_α is the upper α quantile of the standard s-normal distribution.

B. Test of Failure Profile Changes

During a manufacturing process, the relative failure frequency of different failure modes may change due to environment changes. Thus, another important property of the failure profile is whether the failure profile changes over time. Given time intervals $(t_1, t_2]$, $t_1 < t_2 \leq \tau$, and $(t_3, t_4]$, $t_3 < t_4 \leq \tau$, a hypothesis test procedure is developed to test whether the failure profiles are different in those two time intervals. The test is defined as

$$H_0 : R(t_1, t_2; \boldsymbol{\theta}) = R(t_3, t_4; \boldsymbol{\theta}) \text{ vs}$$
$$H_1 : R(t_1, t_2; \boldsymbol{\theta}) \neq R(t_3, t_4; \boldsymbol{\theta}). \quad (18)$$

Because $\sum_{k=1}^{K} R_k(t_1, t_2; \boldsymbol{\theta}) = 1$, and $\sum_{k=1}^{K} R_k(t_3, t_4; \boldsymbol{\theta}) = 1$, only the first $K - 1$ components in the failure profile need to be considered in constructing the test statistic. Therefore, the hypothesis test (18) can be rewritten as

$$H_0 : R_k(t_1, t_2; \boldsymbol{\theta}) = R_k(t_3, t_4; \boldsymbol{\theta}) \text{ vs}$$
$$H_1 : R_k(t_1, t_2; \boldsymbol{\theta}) \neq R_k(t_3, t_4; \boldsymbol{\theta}) \quad \text{for } k = 1, \ldots, K - 1.$$
$$(19)$$

Using the logit transformation $g(x)$, the test in (19) can be further transformed as

$$H_0 : g\left[R_k(t_1, t_2; \boldsymbol{\theta})\right] = g\left[R_k(t_3, t_4; \boldsymbol{\theta})\right] \text{ vs}$$
$$H_1 : g\left[R_k(t_1, t_2; \boldsymbol{\theta})\right] \neq g\left[R_k(t_3, t_4; \boldsymbol{\theta})\right] \quad \text{for } k = 1, \ldots, K - 1.$$
$$(20)$$

Let

$$A(t_1, t_2, t_3, t_4, \widehat{\boldsymbol{\theta}})$$
$$= \left\{ g\left[R_1(t_1, t_2; \widehat{\boldsymbol{\theta}})\right], \ldots, g\left[R_{K-1}(t_1, t_2; \widehat{\boldsymbol{\theta}})\right] \right\}^T$$
$$- \left\{ g\left[R_1(t_3, t_4; \widehat{\boldsymbol{\theta}})\right], \ldots, g\left[R_{K-1}(t_3, t_4; \widehat{\boldsymbol{\theta}})\right] \right\}^T$$
$$= \left[A_1(t_1, t_2, t_3, t_4, \widehat{\boldsymbol{\theta}}), \ldots A_{K-1}(t_1, t_2, t_3, t_4, \widehat{\boldsymbol{\theta}})\right]^T \quad (21)$$

where $A_k(t_1, t_2, t_3, t_4, \widehat{\boldsymbol{\theta}}) = g[R_k(t_1, t_2; \widehat{\boldsymbol{\theta}})] - g[R_k(t_3, t_4; \widehat{\boldsymbol{\theta}})]$.
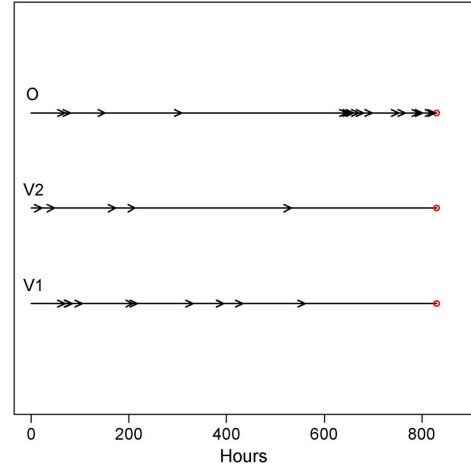

Fig. 3. Event plot of the failure-time data of the HTS system with multiple failure modes (arrows represent events, circles represent the last follow-up time).

Define the test statistic B as

$$B = A(t_1, t_2, t_3, t_4, \widehat{\boldsymbol{\theta}})^T \left\{ Var\left[A(t_1, t_2, t_3, t_4, \widehat{\boldsymbol{\theta}})\right] \right\}^{-1}$$
$$\times A(t_1, t_2, t_3, t_4, \widehat{\boldsymbol{\theta}}) \quad (22)$$

in which $Var[A(t_1, t_2, t_3, t_4, \widehat{\boldsymbol{\theta}})]$ can be obtained by the delta method, i.e.,

$$Var\left[A(t_1, t_2, t_3, t_4, \widehat{\boldsymbol{\theta}})\right]$$
$$= \left[\frac{\partial A(t_1, t_2, t_3, t_4, \widehat{\boldsymbol{\theta}})}{\partial \widehat{\boldsymbol{\theta}}}\right]^T \Sigma(\widehat{\boldsymbol{\theta}}) \left[\frac{\partial A(t_1, t_2, t_3, t_4, \widehat{\boldsymbol{\theta}})}{\partial \widehat{\boldsymbol{\theta}}}\right]. \quad (23)$$

In particular, $\partial A(t_1, t_2, t_3, t_4, \widehat{\boldsymbol{\theta}})/\partial \widehat{\boldsymbol{\theta}} = [\partial A_1(t_1, t_2, t_3, t_4, \widehat{\boldsymbol{\theta}})/\partial \widehat{\boldsymbol{\theta}}, \cdots, \partial A_{K-1}(t_1, t_2, t_3, t_4, \widehat{\boldsymbol{\theta}})/\partial \widehat{\boldsymbol{\theta}}]$, and

$$\frac{\partial A_k(t_1, t_2, t_3, t_4, \widehat{\boldsymbol{\theta}})}{\partial \widehat{\boldsymbol{\theta}}} = \frac{\partial R_k(t_1, t_2; \widehat{\boldsymbol{\theta}})/\partial \widehat{\boldsymbol{\theta}}}{R_k(t_1, t_2; \widehat{\boldsymbol{\theta}}) \left[1 - R_k(t_1, t_2; \widehat{\boldsymbol{\theta}})\right]}$$
$$- \frac{\partial R_k(t_3, t_4; \widehat{\boldsymbol{\theta}})/\partial \widehat{\boldsymbol{\theta}}}{R_k(t_3, t_4; \widehat{\boldsymbol{\theta}}) \left[1 - R_k(t_3, t_4; \widehat{\boldsymbol{\theta}})\right]}.$$

The calculation of $\partial R_k(t_1, t_2; \hat{\boldsymbol{\theta}})/\partial \hat{\boldsymbol{\theta}}$ is the same as in Section IV-A, which is provided in the Appendix. Proposition 2 as follows gives the decision rule to test the hypothesis (20). The detailed proof is provided in the Appendix.

Proposition 2: The hypothesis test in (20) is rejected if $B > \chi^2_{K-1}(\alpha)$, where $\chi^2_{K-1}(\alpha)$ is the $1 - \alpha$ quantile of the χ^2 distribution with degree $K - 1$.

V. APPLICATIONS

A. Application of Failure Profile in High Throughput Screening Automation Systems

In most pharmaceutical and biotechnology companies, HTS is a central function in the drug-discovery process [21]. HTS
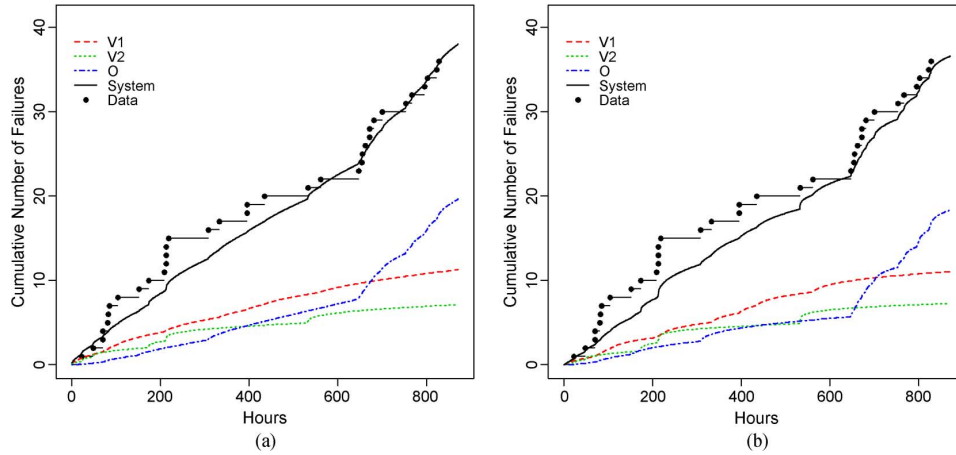
Fig. 4. TRP model fitting results with power law trend function, and different renewal distributions. (a) Weibull. (b) Lognormal.

TABLE I
PARAMETER ESTIMATES, LARGE-SAMPLE STANDARD ERROR, AND APPROXIMATE 95% CIS FOR THE TRP
IN WHICH THE POWER LAW TREND FUNCTION AND THE WEIBULL RENEWAL DISTRIBUTION ARE USED

Failure Mode	Parameter	Estimates	Standard Error	approximate 95% CI	
				Lower	Upper
V1	β	0.789	0.322	0.355	1.755
	η	43.487	58.196	3.157	599.042
	σ	1.328	0.353	0.788	2.237
V2	β	1.523	1.258	0.301	7.689
	η	397.329	513.664	31.531	5006.743
	σ	2.926	1.476	1.089	7.864
O	β	2.070	0.594	1.180	3.631
	η	203.998	92.125	84.185	494.333
	σ	1.580	0.283	1.113	2.244

is the testing of large numbers of candidate molecules in a biological assay. The objective of all HTS laboratories is to test potentially active compounds quickly, and in the most cost effective manner possible. The reliability of the HTS automation system plays a crucial role on the throughput, effectiveness, and cost of HTS processes. Major subsystems in HTS automation include liquid handling, transportation, and reader systems. Numerous robots, computers, software, and other instruments are used in each system. With the constant increase of equipment complexity, it is important to analyze system failure modes to quickly pinpoint the bottleneck problems, and improve the effectiveness of preventive maintenance for the automation system.

Fig. 3 shows the failure-time data collected during a one-year time period from an HTS system of a pharmaceutical company in the United States. The time scale of the failure time is hours in operation. Three failure modes are considered in this study: failure modes O, V1, and V2.

Failure Profile Estimation based on TRP Model: Given the failure-time data of the HTS system, a statistical model is established based on the TRP. With the specification of trend function $\Lambda(\cdot)$, and renewal distribution F, one can fit the data, and obtain the estimates of $\boldsymbol{\theta}$ by maximizing the likelihood function

(10). Fig. 4(a) and (b) illustrate the model fitting results when the trend function is chosen as a power law function, and the renewal distributions are chosen as Weibull, and lognormal, respectively. Under each situation, different parameter values are used for different failure modes. The step segments in each subfigure represent the counting process $N_k(t)$ for failure mode k (i.e., failure modes O, V1, and V2), and $N(t)$ for all failure modes. The lines show the estimates of $\tilde{\Gamma}_k(0, t; \hat{\boldsymbol{\theta}}_k)$ for each failure mode k, as well as $\tilde{\Gamma}(0, t; \hat{\boldsymbol{\theta}}) = \sum_{k=1}^{K} \tilde{\Gamma}_k(0, t; \hat{\boldsymbol{\theta}}_k)$ for all failure modes.

In the literature, likelihood values are generally used to compare different models for model fitting. For TRP models with power law trend functions, the likelihood value is -171.547 when the renewal distribution is the Weibull, and the likelihood value is -173.812 when the renewal distribution is lognormal. As the TRP model with a Weibull renewal distribution fits the data better, this TRP model is chosen for the estimates of the failure profile and the hypothesis testing in this study. Table I lists the parameter estimates, large-sample standard error, and approximate 95% CIs for the TRP. Note that only one estimated parameter (i.e., $\hat{\sigma}$) is listed in Table I for the Weibull distribution.

Fig. 5 illustrates the estimated failure profile $R(t_1, t_2; \hat{\boldsymbol{\theta}})$, where t_1 is fixed at zero, and t_2 changes from zero to τ. From
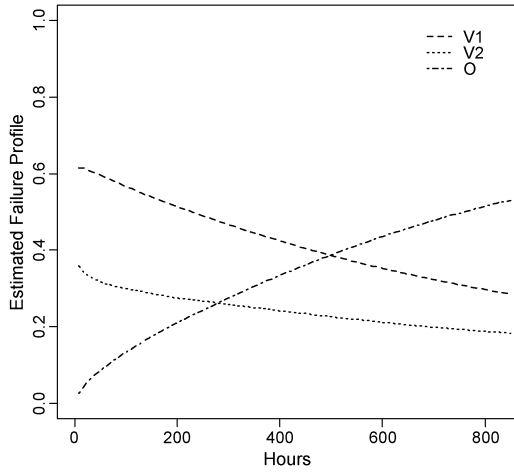
Fig. 5.   Estimated failure profile $R(0, t, \hat{\boldsymbol{\theta}})$ using the TRP model in which the power law trend function and the Weibull renewal distribution are used.
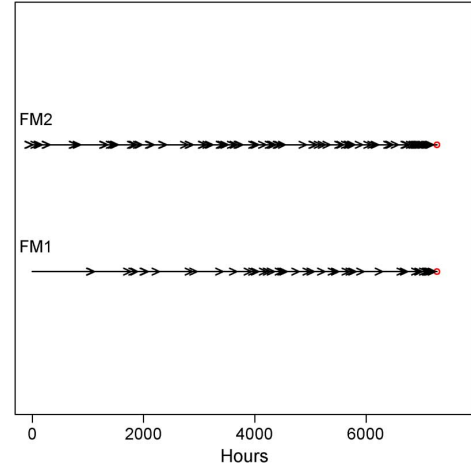

Fig. 6.   Event plot of the failure-time data of the cylinder head production process with two failure modes (arrows represent events, circles represent the last follow-up time).

Fig. 5, it can be seen that the relative failure frequency of the failure mode O keeps increasing over the observation period, while the relative failure frequency for failure modes V1 and V2 decreases over the observation period.

Hypothesis Tests for Failure Profiles in HTS: During the HTS process, there is a significant system environment change at 531.46 hours, when the system was moved to another operating environment. In this section, hypothesis tests are performed to test whether any dominating failure mode exists before and after the environment change, and whether the failure profile changes when the environment changes.

First, to test whether a dominating failure mode exists in time interval (0, 531.46], the test procedure in (16) is applied with t_1, and t_2 being set to 0, and 531.46, respectively. Failure mode V1 is tested for supremacy. The failure profile $R(0, 531.46; \hat{\boldsymbol{\theta}})$ is calculated using the estimated parameters of the TRP model listed in Table I, and the value equals $(0.3777, 0.2208, 0.4015)^T$. As the p-value equals 0.5542, there is no statistical evidence that failure mode V1 is larger than that of other failure modes V2 and O. Similarly, for time interval (531.46, 829.81], $t_1 = 531.46$, and $t_2 = 829.81$. Failure mode O is tested for supremacy. The estimated failure profile $R(531.46, 829.81; \hat{\boldsymbol{\theta}})$ equals $(0.1858, 0.1402, 0.6740)^T$, and the p-value is 0.0055. Thus, the relative failure frequency of failure mode O is statistically larger than that of failure modes V1 and V2.

Second, the hypothesis test (20) is used to test whether the failure profile changes when the environment changes, where t_1, t_2, t_3, and t_4 are set to 0, 531.46, 531.46, and 829.81, respectively. The statistic B is calculated based on (22), and the value of B equals 6.94 with a p-value of 0.031. Based on Proposition 2, the hypothesis H_0 in (20) is rejected. Thus there exists a significant change in the failure profile when the environment changes. This result is consistent with the results in Fig. 5, i.e., the relative failure frequency of failure mode O keeps increasing during the observation period.

Based on the results of statistical tests, we conclude that the HTS system experienced a significant change when the environment changed. As the relative failure frequency of failure

mode O is s-larger than that of failure modes V1 and V2, failure mode O is the bottleneck of the system. After investigation of the system, we find that the corresponding station of mode O tends to experience more failures in the new environment. Thus, it is suggested that components that are more reliable need to be used for the maintenance or repair actions for failure mode O.

B. Application of Failure Profile Analysis in Cylinder Head Production Process

In another case study, a cylinder head is produced after going through sequential stations. The functions of these stations include stamping, applying sealant on taper and cup plugs, installing taper and cup plugs, leak testing, etc. Fig. 6 shows the failure-time data of two stations collected from a cylinder head production process in a United States automotive power-train plant for one and a half years. In this process, it is important to analyze system failure modes to quickly pinpoint the system bottlenecks, and reduce process downtime.

Failure Profile Estimation based on TRP Model: Fig. 7(a) and (b) illustrate the model fitting results when the trend function of the TRP model is chosen as power law function, and the renewal distributions of the TRP model are chosen as Weibull and lognormal, respectively. Under each situation, different parameter values are used for different failure modes.

For TRP models with power law trend functions, the likelihood value is -881.786 when the renewal distribution is Weibull, and the likelihood value is -902.462 when the renewal distribution is lognormal. As the TRP model with Weibull renewal distribution fits the data better, it is chosen for the estimates of the failure profile and the hypothesis testing in this study. Table II lists the parameter estimates, large-sample standard error, and approximate 95% CIs for the TRP in which the trend function is chosen to be power law, and the Weibull is the renewal distribution.

Fig. 8 illustrates the estimated failure profile $R(t_1, t_2; \hat{\boldsymbol{\theta}})$, where t_1 is fixed at zero, and t_2 changes from zero to τ. From
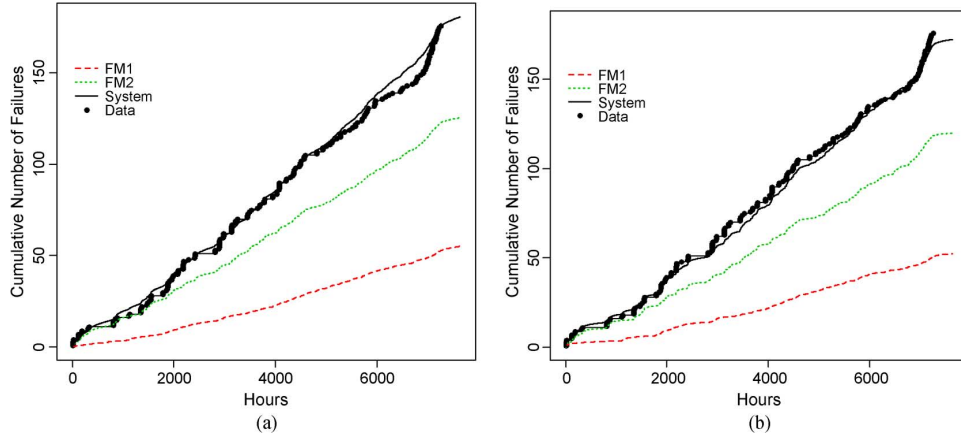
Fig. 7. TRP model fitting results with power law trend function and different renewal distributions. (a) Weibull. (b) Lognormal.

TABLE II
PARAMETER ESTIMATES, LARGE-SAMPLE STANDARD ERROR, AND APPROXIMATE 95% CIs FOR THE TRP
IN WHICH THE POWER LAW TREND FUNCTION AND THE WEIBULL RENEWAL DISTRIBUTION ARE USED

Failure Mode	Parameter	Estimates	Standard Error	approximate 95% CI	
				Lower	Upper
FM1	β	1.156	0.267	0.736	1.817
	η	246.826	203.933	48.878	1246.431
	σ	1.561	0.177	1.249	1.949
FM2	β	0.971	0.141	0.731	1.291
	η	54.906	40.737	12.825	235.053
	σ	1.822	0.132	1.579	2.101

Fig. 8, it can be seen that the relative failure frequency for the failure mode FM2 is always larger than for failure mode FM1.

Hypothesis Tests for Failure Profiles in Cylinder Head Production Process: There are four maintenance times 2808, 5121, 5688, and 6330; and the last follow up time is 7270. The estimated failure profiles are $R(0, 2808; \hat{\boldsymbol{\theta}}) = (0.2700, 0.7300)^T$,

$$R(2808, 5121; \hat{\boldsymbol{\theta}}) = (0.3156, 0.6844)^T,$$
$$R(5121, 5688; \hat{\boldsymbol{\theta}}) = (0.3284, 0.6716)^T,$$
$$R(5688, 6330; \hat{\boldsymbol{\theta}}) = (0.3333, 0.6667)^T,$$
$$\text{and } R(6330, 7270; \hat{\boldsymbol{\theta}}) = (0.3384, 0.6616)^T.$$

The p-values for the supremacy tests for those periods are all less than 0.001. Thus, failure mode FM2 is the dominating failure mode. As the p-values for the failure profile change are all larger than 0.3, there is no significant change in the failure profile over

the observation periods. Because failure mode FM2 is *s*-larger than that of failure modes FM1, more resources need to be allocated to the corresponding station of FM2 to improve its reliability and maintainability.

VI. SUMMARY

In this paper, the failure profile and its statistical properties are investigated when applying the TRP model for repairable systems with multiple failure modes. The failure profile is analyzed using failure-time data collected from a single repairable system with multiple failure modes. The TRP model provides a versatile tool for modeling failure profiles of single repairable systems with competing risks. In addition, hypothesis testing procedures are developed to analyze statistical properties of failure profiles. The proposed methodology is illustrated using two case studies. One is an HTS automation system for drug discovery

$$\frac{\partial R_k(t_1, t_2; \boldsymbol{\theta})}{\partial \boldsymbol{\theta}} = \frac{(\partial \Gamma_k(t_1, t_2; \boldsymbol{\theta}_k)/\partial \boldsymbol{\theta}) \times \sum_{j=1}^{K} \Gamma_j(t_1, t_2; \boldsymbol{\theta}_j) - \Gamma_k(t_1, t_2; \boldsymbol{\theta}_k) \times \sum_{j=1}^{K} (\partial \Gamma_j(t_1, t_2; \boldsymbol{\theta}_j)/\partial \boldsymbol{\theta})}{\left[\sum_{j=1}^{K} \Gamma_j(t_1, t_2; \boldsymbol{\theta}_j)\right]^2}.$$
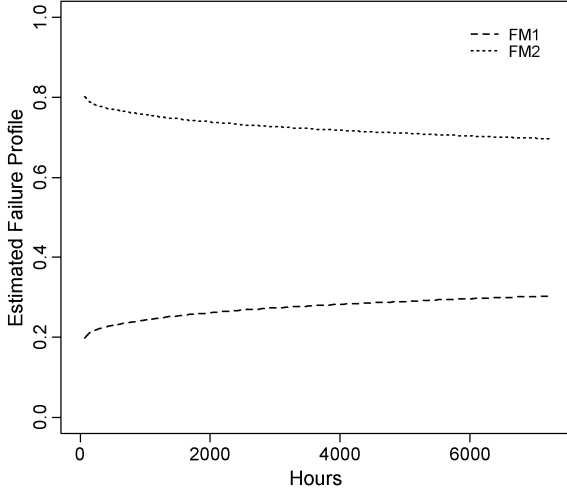
Fig. 8. Estimated failure profile $R(0, t, \hat{\boldsymbol{\theta}})$ using the TRP model with the power law trend function, and the Weibull renewal distribution.

from the pharmaceutical industry, and the other is a cylinder head manufacturing process.

As future research, on-line change points detection of the failure profile for single repairable systems can be investigated, which can expedite the process correction decision. Another interesting research topic is to obtain an optimal maintenance resource allocation based on the results of failure profile analysis.

APPENDIX A

A. Proof of Proposition 1

Let $Z_{k,j} = D_{k,j}(t_1, t_2; \widehat{\boldsymbol{\theta}}) / \{\operatorname{Var}[D_{k,j}(t_1, t_2; \widehat{\boldsymbol{\theta}})]\}^{1/2}$. The quantity $Z_{k,j}$ is approximately standard s-normal distributed under the boundary of the null hypothesis $H_{0,j}$ (i.e., $R_k(t_1, t_2; \boldsymbol{\theta}) = R_j(t_1, t_2; \boldsymbol{\theta})$). That is, $Z_{k,j} \stackrel{.}{\sim} N(0, 1)$ when $R_k(t_1, t_2; \boldsymbol{\theta}) = R_j(t_1, t_2; \boldsymbol{\theta})$. The asymptotic variance of $D_{k,j}(t_1, t_2; \widehat{\boldsymbol{\theta}})$ is obtained by using the delta method, which is a widely-used approach to obtain the variance of functions of estimators (see Appendix B.2 in [15] for details on the delta method). In particular, $\operatorname{Var}[D_{k,j}(t_1, t_2; \widehat{\boldsymbol{\theta}})] = [\partial D_{k,j}(t_1, t_2; \widehat{\boldsymbol{\theta}})/\partial \widehat{\boldsymbol{\theta}}]^T \Sigma(\widehat{\boldsymbol{\theta}})[\partial D_{k,j}(t_1, t_2; \widehat{\boldsymbol{\theta}})/\partial \widehat{\boldsymbol{\theta}}]$. Here, $\Sigma(\widehat{\boldsymbol{\theta}}) = I^{-1}(\widehat{\boldsymbol{\theta}})$ is the large-sample approximate variance covariance matrix for $\widehat{\boldsymbol{\theta}}$, and $I(\widehat{\boldsymbol{\theta}})$ is defined as in (11). In addition,

$$\frac{\partial D_{k,j}(t_1, t_2; \widehat{\boldsymbol{\theta}})}{\partial \widehat{\boldsymbol{\theta}}} = \frac{\partial R_k(t_1, t_2; \widehat{\boldsymbol{\theta}})/\partial \widehat{\boldsymbol{\theta}}}{R_k(t_1, t_2; \widehat{\boldsymbol{\theta}}) \left[1 - R_k(t_1, t_2; \widehat{\boldsymbol{\theta}})\right]} - \frac{\partial R_j(t_1, t_2; \widehat{\boldsymbol{\theta}})/\partial \widehat{\boldsymbol{\theta}}}{R_j(t_1, t_2; \widehat{\boldsymbol{\theta}}) \left[1 - R_j(t_1, t_2; \widehat{\boldsymbol{\theta}})\right]}.$$

Thus, $W_{k,j} = Z_{k,j}$, which has an approximate standard s-normal distribution under the boundary of the null hypothesis. Therefore, Proposition 1 holds.

B. Proof of Proposition 2

The ML estimator $\hat{\boldsymbol{\theta}}$ is asymptotically distributed with multivariate normal $N[\boldsymbol{\theta}, \Sigma(\hat{\boldsymbol{\theta}})]$. In addition, $A(t_1, t_2, t_3, t_4, \boldsymbol{\theta})$ is a function of $\boldsymbol{\theta}$, thus $A(t_1, t_2, t_3, t_4, \widehat{\boldsymbol{\theta}})$ is asymptotically distributed with $K - 1$ multivariate normal $N\{A(t_1, t_2, t_3, t_4, \boldsymbol{\theta}), Var[A(t_1, t_2, t_3, t_4, \widehat{\boldsymbol{\theta}})]\}$. Based on the distribution theory of the quadratic form of the multivariate normal distribution, the test statistic B in (22) approximately has a distribution of χ^2_{K-1} with $K - 1$ degrees of freedom under the null hypothesis. Hence, the hypothesis test in (20) is rejected if $B > \chi^2_{K-1}(\alpha)$.

C. Calculation of $\partial R_k(t_1, t_2; \hat{\boldsymbol{\theta}})/\partial \hat{\boldsymbol{\theta}}$

Note that $\partial R_k(t_1, t_2; \hat{\boldsymbol{\theta}})/\partial \hat{\boldsymbol{\theta}} = \partial R_k(t_1, t_2; \boldsymbol{\theta})/\partial \boldsymbol{\theta}|_{\boldsymbol{\theta}=\hat{\boldsymbol{\theta}}}$. To calculate $\partial R_k(t_1, t_2; \boldsymbol{\theta})/\partial \boldsymbol{\theta}$, shown at the bottom of the previous page, We only need to calculate $\partial \Gamma_k(t_1, t_2; \boldsymbol{\theta}_k)/\partial \boldsymbol{\theta}$. Based on the TRP model, $\partial \Gamma_k(t_1, t_2; \boldsymbol{\theta}_k)/\partial \boldsymbol{\theta} = \mathbf{E}(\int_{t_1}^{t_2}[\partial \gamma_k(s; \boldsymbol{\theta}_k)/\partial \boldsymbol{\theta}]ds)$, and

$$\frac{\partial \gamma_k(t; \boldsymbol{\theta}_k)}{\partial \boldsymbol{\theta}}$$
$$= h_z \left[\Lambda(t; \boldsymbol{\theta}_{\lambda_k}) - \Lambda\left(T_{k, N_k(t^-)}; \boldsymbol{\theta}_{\lambda_k}\right); \boldsymbol{\theta}_{F_k}\right]$$
$$\times \left[\int_0^t \frac{\partial \lambda(s; \boldsymbol{\theta}_{\lambda_k})}{\partial \boldsymbol{\theta}} ds - \int_0^{T_{k, N_k(t^-)}} \frac{\partial \lambda(s; \boldsymbol{\theta}_{\lambda_k})}{\partial \boldsymbol{\theta}} ds\right] \lambda(t; \boldsymbol{\theta}_{\lambda_k})$$
$$+ h_F \left[\Lambda(t; \boldsymbol{\theta}_{\lambda_k}) - \Lambda\left(T_{k, N_k(t^-)}; \boldsymbol{\theta}_{\lambda_k}\right); \boldsymbol{\theta}_{F_k}\right] \lambda(t; \boldsymbol{\theta}_{\lambda_k})$$
$$+ h \left[\Lambda(t; \boldsymbol{\theta}_{\lambda_k}) - \Lambda\left(T_{k, N_k(t^-)}; \boldsymbol{\theta}_{\lambda_k}\right); \boldsymbol{\theta}_{F_k}\right] \frac{\partial \lambda(t; \boldsymbol{\theta}_{\lambda_k})}{\partial \boldsymbol{\theta}}.$$

Here, $h_z(z; \boldsymbol{\theta}_{F_k}) = dh(z; \boldsymbol{\theta}_{F_k})/dz$, and $h_F(z; \boldsymbol{\theta}_{F_k}) = \partial h(z; \boldsymbol{\theta}_{F_k})/\partial \boldsymbol{\theta}_{F_k}$. As the intensity function for the power law relationship is $\lambda(t; \boldsymbol{\theta}_\lambda) = (\beta/\eta)(t/\eta)^{\beta-1}$, $\partial \lambda(t; \boldsymbol{\theta}_\lambda)/\partial \beta = \eta^{-\beta}t^{\beta-1}[1 - \beta\log(\eta) + \beta\log(t)]$ and $\partial \lambda(t; \boldsymbol{\theta}_\lambda)/\partial \eta = -\beta^2 \eta^{-(\beta+1)}t^{\beta-1}$. For the Weibull distribution, the hazard function is $h(z; \boldsymbol{\theta}_F) = e^{-(\mu/\sigma)}z^{1/\sigma}$, and $h_z(z; \boldsymbol{\theta}_F)$ can be calculated as $(1/\sigma)e^{-(\mu/\sigma)}z^{((1/\sigma)-1)}$. The calculation of $h_F(z; \boldsymbol{\theta}_F)$ for the Weibull distribution, however, is not straightforward because μ is also a function of σ due to the mean restriction on the renewal distribution. Numerical derivatives can be used here. Similar results can also be obtained for the lognormal distribution.

REFERENCES

[1] S. E. Rigdon and A. P. Basu, *Statistical Methods for the Reliability of Repairable Systems.* New York: Wiley, 2000.
[2] D. R. Cox, "The statistical analysis of dependencies in point processes," *Stochastic Point Processes: Statistical Analysis, Theory, and Applications*, pp. 55–66, 1972.
[3] M. Berman, "Inhomogeneous and modulated gamma processes," *Biometrika*, vol. 68, no. 1, pp. 143–152, 1981.
[4] M. J. Lakey and S. E. Rigdon, "The modulated power law process," in *Proceedings of the 45th Annual Quality Congress*, Milwaukee, WI, USA, 1992, pp. 559–563.

[5] B. H. Lindqvist, G. Elvebakk, and K. Heggland, "The trend-renewal process for statistical analysis of repairable systems," *Technometrics*, vol. 45, no. 1, pp. 31–44, 2003.

[6] H. Langseth and B. H. Lindqvist, "The modulated power law process," in *Proceedings of the 45th Annual Quality Congress*, Milwaukee, 1992, pp. 559–563.

[7] M. Kijima, "Some results for repairable systems with general repair," *Journal of Applied Probability*, vol. 26, no. 1, pp. 89–102, 1989.

[8] L. Doyen and O. Gaudoin, "Classes of imperfect repair models based on reduction of failure intensity or virtual age," *Reliability Engineering & System Safety*, vol. 84, no. 1, pp. 45–56, 2004.

[9] M. Shaked and J. G. Shanthikumar, "Multivariate imperfect repair," *Operations Research*, vol. 34, no. 3, pp. 437–448, 1986.

[10] T. Bedford and B. H. Lindqvist, "The identifiability problem for repairable systems subject to competing risks," *Advances in Applied Probability*, vol. 36, no. 3, pp. 774–790, 2004.

[11] H. Langseth and B. H. Lindqvist, "A maintenance model for components exposed to several failure mechanisms and imperfect repair," in *Mathematical and Statistical Methods in Reliability*, B. H. Lindqvist and K. A. Doksum, Eds. River Edge: World Scientific, 2003, pp. 415–430.

[12] L. Doyen and O. Gaudoin, "Imperfect maintenance in a generalized competing risks framework," *Journal of Applied Probability*, vol. 43, no. 3, pp. 825–839, 2006.

[13] B. H. Lindqvist, "On the statistical modeling and analysis of repairable systems," *Statistical science*, vol. 21, no. 4, pp. 532–551, 2006.

[14] M. A. Friedman, "Applications of Hazard Rate Profile to Software Reliability Prediction, Growth Modeling and Allocation," *Quality and Reliability Engineering International*, vol. 8, no. 5, pp. 413–418, 1992.

[15] W. Q. Meeker and L. A. Escobar, *Statistical Methods for Reliability Data*. Hoboken: Wiley, 1998.

[16] A. Tsiatis, "A nonidentifiability aspect of the problem of competing risks," *Proceedings of the National Academy of Sciences of the United States of America*, vol. 72, no. 1, pp. 20–22, 1975.

[17] P. K. Andersen, *Statistical Models Based on Counting processes*. New York: Springer-Verlag, 1993.

[18] Å. Svensson, "Asymptotic estimation in counting processes with parametric intensities based on one realization," *Scandinavian Journal of Statistics*, vol. 17, no. 1, pp. 23–33, 1990.

[19] G. Casella and R. L. Berger, *Statistical Inference*, second ed. Pacific Grove: Duxbury Press, 2001.

[20] M. J. Silvapulle and P. K. Sen, *Constrained Statistical Inference: Inequality, Order, and Shape Restrictions*. Hoboken: Wiley, 2004.

[21] R. Macarron and R. P. Hertzberg, "Design and implementation of high throughput screening assays," *Molecular Biotechnology*, vol. 47, no. 3, pp. 270–285, 2009.

Qingyu Yang received the B.S., and M.S. degrees in Automatic Control and Intelligent System from the University of Science and Technology of China in 2000, and 2003 respectively; and the M.S. degree in Statistics, and the Ph.D. degree in Industrial Engineering, from the University of Iowa in 2007, and 2008 respectively. Currently, he is an Assistant Professor in the Department of Industrial and System Engineering at Wayne State University. His research interests include statistical data analysis, complex system modeling, and system informatics. He is a member of INFORMS and IIE.

Yili Hong received a B.S. in statistics (2004) from the University of Science and Technology of China; and M.S., and Ph.D. degrees in statistics (2005, 2009) from Iowa State University. He is currently an Assistant Professor in the Department of Statistics at Virginia Tech. His research interests include reliability data analysis, and engineering statistics.

Yong Chen is currently an associate professor in the Department of Mechanical and Industrial Engineering at the University of Iowa. He received the B.E. degree in computer science from Tsinghua University, China in 1998; and the Master degree in Statistics, and Ph.D. degree in Industrial & Operations Engineering, both from the University of Michigan in 2003. His research interests include quality and reliability engineering, pattern recognition, applied statistics, and simulation optimization. He is a member of INFORMS, the ASA, and the IMS.

Jianjun Shi is Carolyn J. Stewart Chair Professor at H. Milton Stewart School of Industrial and Systems Engineering, Georgia Institute of Technology. Before joined Georgia Tech in 2008, he was the G. Lawton and Louise G. Johnson Professor of Engineering at the University of Michigan. He got his B.S., and M.S. in Electrical Engineering at the Beijing Institute of Technology in 1984, and 1987 respectively; and his Ph.D. in Mechanical Engineering at the University of Michigan in 1992.

Professor Shi's research interests focus on the fusion of advanced statistics, signal processing, control theory, and domain knowledge to develop methodologies for modeling, monitoring, diagnosis, and control for complex systems in a data rich environment. Professor Shi is the founding chairperson of the Quality, Statistics and Reliability (QSR) Subdivision at INFORMS. He currently serves as the Focus Issue Editor of IIE Transactions on Quality and Reliability Engineering. He is a Fellow of the Institute of Industrial Engineering (IIE), a Fellow of American Society of Mechanical Engineering (ASME), and a Fellow of Institute of Operations Research and Management Science (INFORMS), and also a life member of ASA.